Theoretical Study of Al_n and Al_nO ($n = 2-10$) Clusters

Jiao Sun, Wen Cai Lu, Hong Wang, Ze-Sheng Li,* and Chia-Chung Sun

State Key Lab of Theoretical and Computational Chemistry, Institute of Theoretical Chemistry, Jilin University, Changchun 130023, People's Republic of China

Received: March 1, 2005; In Final Form: October 4, 2005

The stable structures, energies, and electronic properties of neutral, cationic, and anionic clusters of Al_n ($n = 2-10$) are studied systematically at the B3LYP/6-311G(2d) level. We find that our optimized structures of Al_5^+, Al_9^+, Al_9^-, Al_{10}, Al_{10}^+, and Al_{10}^- clusters are more stable than the corresponding ones proposed in previous literature reports. For the studied neutral aluminum clusters, our results show that the stability has an odd/even alternation phenomenon. We also find that the Al_3, Al_7, Al_7^+, and Al_7^- structures are more stable than their neighbors according to their binding energies. For Al_7^+ with a special stability, the nucleus-independent chemical shifts and resonance energies are calculated to evaluate its aromaticity. In addition, we present results on hardness, ionization potential, and electron detachment energy. On the basis of the stable structures of the neutral Al_n ($n = 2-10$) clusters, the Al_nO ($n = 2-10$) clusters are further investigated at the B3LYP/6-311G(2d), and the lowest-energy structures are searched. The structures show that oxygen tends to either be absorbed at the surface of the aluminum clusters or be inserted between Al atoms to form an $Al_{n-1}OAl$ motif, of which the Al_{n-1} part retains the stable structure of pure aluminum clusters.

Introduction

Aluminum clusters have been of great scientific interest in the past 20 years. Such attention is due to the special status of aluminum materials as well as the possible development of cluster-based materials.[1] The interaction of oxygen with aluminum is a universal reaction, and aluminum oxides are very important ceramic materials that have many technological applications. Understanding the mechanism of oxygen atoms reacting with aluminum is important because it can provide useful information in many research fields such as surface science and catalysis related to aluminum.[2]

Some neutral and ionic clusters of Al_n ($n = 1-15$) have been studied theoretically[3−10] and experimentally.[11−16] Al_7^+ and Al_{13}^- were considered to be the magic clusters as they contain 20 and 40 valence electrons, respectively. They exhibit special behaviors in experiments. For example, Al_{13} acts as a superhalogen, and it and its conformers have been extensively investigated.[7] Moreover, the intensities of the peaks in the mass spectra of clusters indicate that Al_7^+, with a special stability, is a magic cluster because of an unusually large peak.[13] Similarly, Al_3^+ has a closed-shell structure with eight valence electrons. However, the conclusion that Al_3^+ is a magic cluster has met with conflict.[6,13,14] Whereas one group observed that Al_3^+ is dominant in photodestruction experiments,[13] another group reported no finding of Al_3^+ in collision-induced fragmentation.[14]

Recently, aromaticity has become a rapid-developing area of investigation. The concept of aromaticity has been extended from organic to inorganic systems, and ciiteria and indices of aromaticity have also been developed. One can show the aromaticity of a system from several aspects, such as delocalized molecular orbitals, nucleus-independent chemical shift (NICS) values, resonance energies, and absolute hardness. Li et al. used aromaticity to interpret the stability of the all-metal structural unit Al_4^{2-} having two delocalized π electrons.[17] Zhan et al.[18] further suggested that the Al_4^{2-} structure could have an unusual multifold aromaticity of one π and two σ orbitals, basing their conclusions on calculated wave functions and resonance energies. They also reported that the four valence electrons of Al_3^- were associated with two independent delocalized bonding systems, one π and one σ, in which each delocalized system of multifold aromaticity satisfies the $4n + 2$ electron-counting rule. Kuznetsov et al. discussed the aromaticity of Al_3^- by comparing molecular orbitals (MOs) of Al_3^- and $C_3H_3^+$,[19] and in later work, they also found that the structures and MOs of Al_6^{2-} can be considered as those of two Al_3^- units and explored three-dimensional π and σ aromaticity in Al_6^{2-} and MAl_6^-.[20]

For aluminum oxides, Boldyrev et al. discovered Al_4O, in which the oxygen atom is surrounded by four aluminum atoms in a square-planar (D_{4h}) arrangement. In the hyperaluminum molecule, they believe that the electronic structure, combining ionic and substantial metal−metal bonding, anticipates a large, new class of molecules. Hence, the usual valence theory, which does not include all possible interatomic interactions as bonding possibilities, must be modified.[21] In this article, small $Al_{1-4}O$ clusters were studied. However, this is not sufficient for hyperaluminum clusters.

The oxidation reactions of neutral and ionic aluminum clusters have been extensively investigated in the gas phase.[22−31] Theoretical calculations have been performed for AlO,[32] Al_2O,[33] and neutral and anionic Al_3O_n ($n = 1-8$) clusters.[34−38] For the cases of $n = 0-5$, Wu et al. reported that the electron affinity of neutral clusters increases with increasing oxygen ratio in a systematic study of anion photoelectron spectra.[39,40] In the molecular-dynamics (MD) simulation of the oxidation of an aluminum nanocluster, Campbell et al.[41] reported that aluminum moves outward and oxygen moves toward the interior of the cluster. Then, what about the characters of the Al−O and Al−Al bonds in clusters? This issue might need more attention from both experimental and theoretical studies.

* To whom correspondence should be addressed. E-mail: zeshengli@mail.jlu.edu.cn.

10.1021/jp051033+ CCC: $33.50
Published on Web 02/08/2006

Therefore, it is necessary to confirm and further explain the stable structures of neutral, cationic, and anionic Al_n ($n = 2-10$) clusters and their reactivity behaviors. In this paper, we studied the stable structures and their corresponding properties for Al_n and Al_nO ($n = 2-10$) clusters. For Al_7^+, we attempt to explain its special stabilities according to both the jellium shell closing[42] and multifold aromaticity concepts.[18−20] For Al_nO, we systematically studied the geometries, binding energies, fragmentation energies, electronic structures, and highest occupied molecular orbital (HOMO)−lowest unoccupied molecular orbital (LUMO) gaps to reveal the chemical properties for such types of clusters. These results are compared with experimental data and previous calculations.

Computational Methods

Computations were performed with the Gaussian 03 package.[43] The density functional theory (DFT) of Becker's hybrid three-parameter functional at the Lee, Yang, and Parr correlation functional (B3LYP)[44] level with the 6-311G(2d) basis set is employed for studying the structures of Al_n, Al_n^-, Al_n^+, and Al_nO ($n = 2-10$) species. Different spin multiplicities and initial structures are considered as well. To confirm the stability of structures of both pure aluminum and aluminum oxide clusters, the vibrational frequencies were also analyzed. In addition, the ionization potentials (vertical and adiabatic) and electron detachment energies (vertical and adiabatic) were studied.

Here, cluster aromaticities are evaluated by delocalized MOs, nucleus-independent chemical shifts (NICSs),[45] resonance energies, etc. To denote the property of σ or π aromaticity, the NICS values at the center of the rings or the cages [NICS(0)] and at 1 Å over the ring plane [NICS(1)] were calculated using GIAO[46] at the B3LYP/6-311G(2d) level. The resonance energies were refined using the method CCSD(T)[47−49] and the more extended 6-311+G(2df) basis sets. For aluminum oxide clusters, natural population analyses (NPA) and natural bond orbital (NBO) analyses were performed using the NBO program as implemented in the Gaussian 03 program.[50] The HOMO−LUMO gaps for Al_nO ($n = 2-10$) were obtained from B3LYP/6-311G-(2d) calculations.

Results and Discussion

(A) Al_n Clusters ($n = 2-10$). *(i) Structures.* The stable structures for neutral and ionic Al_{2-10} are shown in Figure 1 while the corresponding energies are given in Table 1. The dimer is one of the well-studied aluminum clusters.[4,6,8,18,21] Zhan et al.[18] determined the ground state, $^3\Pi_u$, and two excited states, $^3\Sigma_g^-$ and $^1\Sigma_g^+$, of Al_2 at CCSD(T)/aug-cc-pVxZ (x = D, T, Q) level. Here, we give two lowest-energy structures of Al_2: one is the ground state $^3\Pi_u$ with a bond length of 2.76 Å, and the other is the excited state $^3\Sigma_g^-$ with a bond length of 2.51 Å, which is 0.114 eV higher in energy than the $^3\Pi_u$ state. The ground state of Al_2^+ has $^2\Sigma_g^+$ symmetry, and its bond length is 3.34 Å. For Al_2^-, the ground state is of $^4\Sigma_g^-$ symmetry with a bond length of 2.59 Å. These results agree well with the previous studies.[6,8,18,21] The optimized geometries of Al_3^+, Al_3, and Al_3^- are all equilateral triangles, in which Al_3 and Al_3^- have almost equal bond lengths of 2.54 Å. Martínez et al. carefully studied Al_4 and Al_4^+ and found that both rhomboidal and square possible stable structures are very close in energy.[10] Our calculated results for Al_4, Al_4^-, and Al_4^+ confirm that the rhomboidal structures with bond angles of 69.4°, 76.3°, and 74.7° for Al_4, Al_4^-, and Al_4^+ are indeed the lowest-energy structures. The present optimized structures of the small Al_n ($n \leq 4$) clusters are in good agreement with the previous calculated results.[3−5,10,18−21]

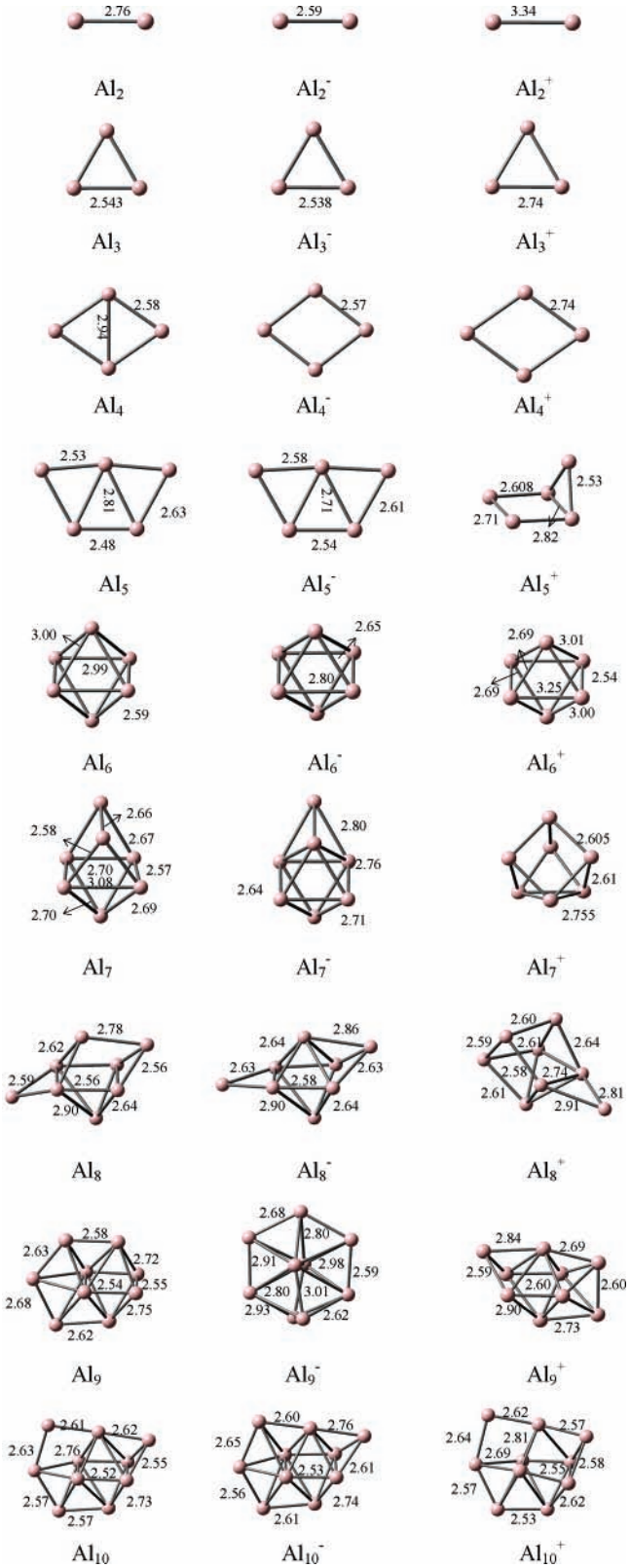

Figure 1. Optimized geometries of neutral and ionic Al_{2-10} clusters (bond lengths in Å).

The structures of Al_5 and Al_5^- are planar with C_{2v} symmetry, whereas the Al_5^+ cluster is a three-dimensional structure with a dihedral angle of 93.6° that is not reported. The structures of neutral and ionic Al_6 are identified as an anomalous octahedral form, in which Al_6^- is more close to an octahedron and thus

TABLE 1: Total Energies[a] (a.u.), Preferred Spin Multiplicities, and Point Groups of Neutral, Cationic, and Anionic Al_{1-10} Clusters

	neutral			cationic			anionic		
n	E_n	mult	group	E_n^+	mult	group	E_n^-	mult	group
1	−242.3863666	2		−242.1650763	1		−242.3949643	3	
2	−484.8207218	3	$D_{\infty h}$	−484.6064149	2	$D_{\infty h}$	−484.8672397	4	$D_{\infty h}$
3	−727.2756992	2	D_{3h}	−727.0458068	3	D_{3h}	−727.3341151	1	D_{3h}
4	−969.7261549	3	D_{2h}	−969.4973449	4	D_{2h}	−969.7007200	2	D_{2h}
5	−1212.1940165	2	C_{2v}	−1211.9644282	1	C_s	**−1212.2682926**	1	C_{2v}
6	−1454.6678743	1	D_{3d}	−1454.4318986	2	C_s	−1454.7509903	2	S_6
7	−1697.1577348	2	C_s	−1696.9513666	1	C_{3v}	**−1697.2315988**	1	C_{3v}
8	**−1939.6138646**	1	C_s	**−1939.3921604**		C_s	**−1939.6916730**	2	C_s
9	**−2182.0757811**	2	C_s	**−2181.8573716**	1	C_s	**−2182.1687090**	1	C_2
10	**−2424.5463384**	1	C_s	**−2424.3276529**	2	C1	**−2424.6347271**	2	C_s

[a] Calculated at the B3LYP/6-311G(2d) level, including zero-point corrections.

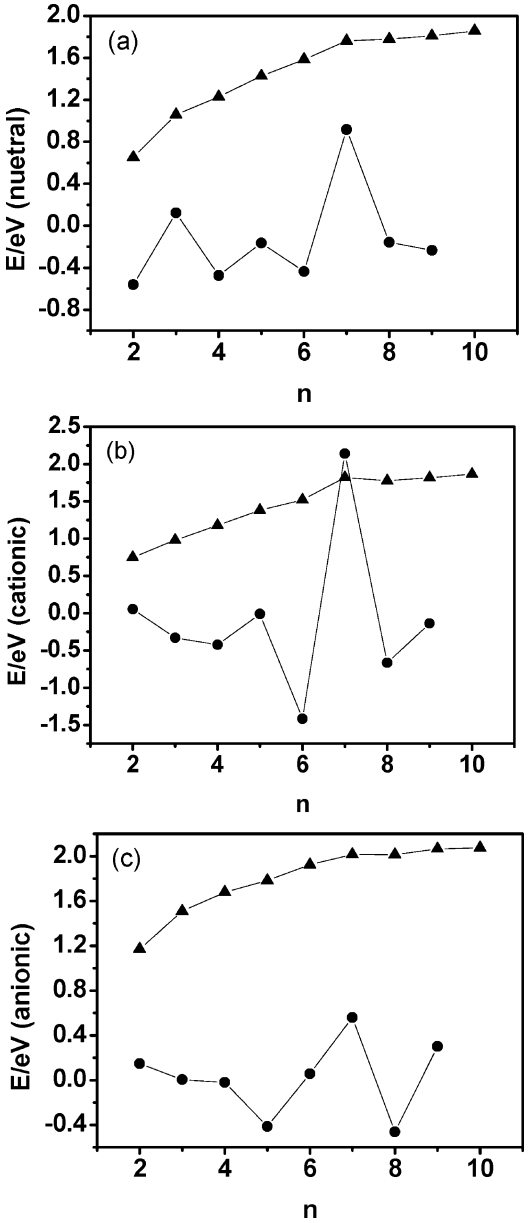

Figure 2. Binding energies (triangles joined by solid line) and second difference in energies (circles joined by solid line) of (a) neutral, (b) cationic, and (c) anionic Al_n ($n = 2-10$) clusters.

more compact. Among neutral and ionic Al_7 species, Al_7^- can be identified as a capped form of the Al_6 structure and has new bonds formed compared to Al_7.

Our results for Al_{8-10} ionic clusters are not in complete agreement with the previous report.[6] Compared to the neutral structure of Al_8, Al_8^- is not much different, whereas Al_8^+ changes significantly in structure. However, the three structures all look like one Al atom connecting to Al_7. Similarly, Al_9^+ can be viewed as an Al atom attached to Al_8. The structure of Al_{10} is a capped form of Al_9. The structure of Al_{10} is almost unaffected by losing or gaining one electron. Our presented structures of Al_{6-9} neutral clusters are in good agreement with the stable structures proposed by Jones.[4,5] For Al_{10}, Jones[4] predicted stable singlet Al_{10} as a capped form of Al_8, using simulated annealing. A similar structure has been reported by Rao et al. at the GGA/LanL2DZ level, but that structure has triplet multiplicity.[6] We performed optimization calculations on the Al_{10} structures in ref 4 and obtained similar structures, in which the lowest-energy structure of singlet Al_{10} is lower than the triplet state by 0.243 eV. In this work, our predicted Al_{10} singlet structure (Figure 1) is 0.167 eV more stable than the triplet, and meanwhile, it is 0.240 eV lower in energy than the singlet Al_{10} structure of ref 4.

TABLE 2: Binding Energies E_b (eV) and Global Hardness Values η (eV) of Neutral, Cationic, and Anionic Al_n ($n = 2-10$) Clusters[a]

	E_b			η		
n	Al_n	Al_n^+	Al_n^-	Al_n	Al_n^+	Al_n^-
2	0.653	0.748	1.169	5.519	5.897	5.080
3	1.058	0.980	1.509	4.826	5.451	4.576
4	1.229	1.178	1.679	4.438	4.799	4.229
5	1.427	1.382	1.784	4.543	4.658	4.006
6	1.586	1.519	1.924	4.635	4.575	4.250
7	1.762	1.820	2.015	4.435	5.609	4.188
8	1.779	1.777	2.014	4.510	4.205	3.857
9	1.809	1.818	2.064	4.134	4.389	3.955
10	1.858	1.865	2.075	4.046	3.992	3.706

[a] Calculated at the B3LYP/6-311G(2d) level.

(ii) Binding Energy and Relative Stability. In Figure 2, we plot curves of the binding energy and second difference in energy for neutral and ionic clusters. The second difference in energy is defined by

$$\Delta^2 E(Al_n) = -2E(Al_n) + E(Al_{n-1}) + E(Al_{n+1}) \qquad (1)$$

As shown in Figure 2, the binding energies for Al_n clusters (neutral and ionic) increase with increasing cluster size. The second differences in energy exhibit a small odd/even alternation in neutral clusters,[7,15] and the conspicuous peaks appear at Al_3, Al_7, Al_7^+, and Al_7^-, indicating that these four clusters are very stable.

For Al_3, the calculation results show that it has a special stability among neutral Al clusters. This stability can be ascribed to the similarities of its bond lengths and electron structure with those of Al_3^-, which has been shown to have aromatic character.

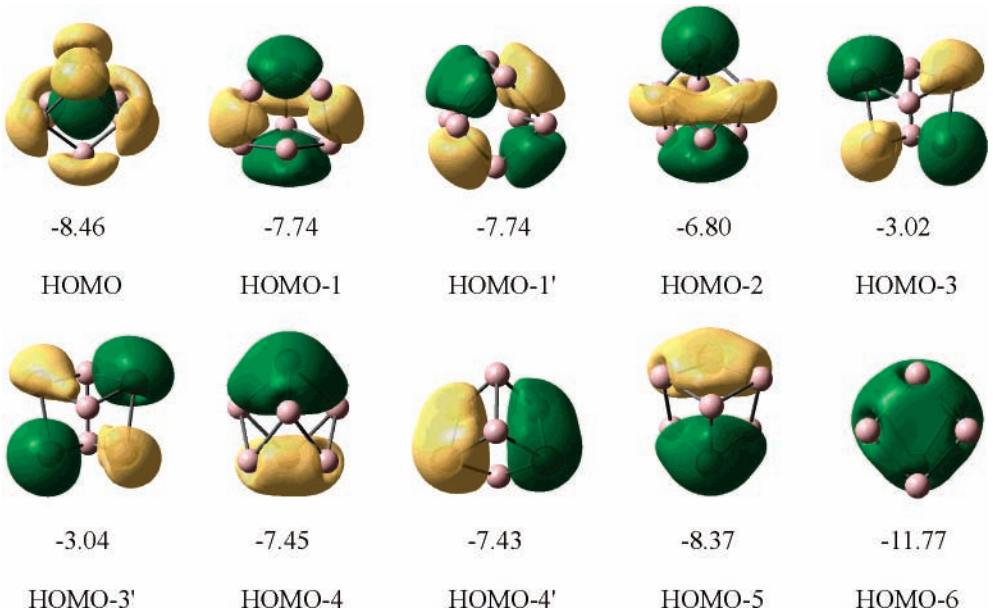

Figure 3. Molecular orbitals (isodensity value is 0.03) and NICS values (ppm) of the Al_7^+ cluster.

According to the jellium model, the atomic arrangements in clusters are not very important in describing their electronic structure.[42] One can approximate a cluster as a spherical distribution of positive ion charge to which the valence electrons respond.[6] Al_3^+ containing eight valence electrons can be considered as a magic cluster; however, its stability has been a topic of debate. In our work, Al_3^+ is not as stable as expected, as its binding energy is only 0.980 eV and its hardness of 5.451 eV is only slightly greater than that of its neighbor clusters (Table 2). The results suggest that Al_3^+ is not very stable, which is consistent with experimental[14] and theoretical[6] studies.

Al_3^- is recognized as having σ and π aromaticity.[8,9] The energetic criterion of aromaticity, i.e., resonance energy (RE), is directly related to the stability of the molecular structure. Following Dewar's approach for calculating RE values,[18,51,52] $RE(Al_3^-)$ can be obtained as

$$RE(Al_3^-) = \Delta E(Al_3^- \rightarrow 3Al + e^-) - 2\Delta E[Al_2(^1\Sigma_g) \rightarrow 2Al] \quad (2)$$

where each Al atom is considered to contribute one 3p bonding electron, so that Al_3^- has two bonding electron pairs. At the CCSD(T)/6-311+G(2df) level of theory, $RE(Al_3^-)$ is calculated to be 76.3 kcal/mol, with a $\Delta E(Al_3^- \rightarrow 3Al + e^-)$ value of 126.5 kcal/mol and an Al_2 dissociation energy, $\Delta E[Al_2(^1\Sigma_g) \rightarrow 2Al]$, of 25.1 kcal/mol. If we use the $\Delta E(Al_3^- \rightarrow 2Al + Al^-)$ (120.0 kcal/mol) and $\Delta E[Al_2(^3\Pi_u) \rightarrow 2Al]$ (31.8 kcal/mol) values, then $RE(Al_3^-)$ is 56.4 kcal/mol. The two calculated results for $RE(Al_3^-)$, 76.3 and 56.4 kcal/mol, as the upper and lower limits, respectively, are in very good agreement with the corresponding values of 79.3 and 56.3 kcal/mol from ref 18 and 56 kcal/mol from ref 20.

Let us discuss the stability of Al_7 and Al_7^+ caged clusters. From the experimental report by Cox et al.,[24] the reactive rate constant of Al_7 with oxygen is a minimum in the reactivity curve. According to the calculated second difference in energy, Al_7 indeed shows a special stability compared to Al_6 and Al_8.

Closed-shell Al_7^+ is an outstanding representative for magic clusters. It has a quite large binding energy (1.820 eV) and the greatest hardness (5.609 eV) of all of the aluminum clusters we have studied except for Al_2^+. Why is the stability of Al_7^+ so much larger? From the molecular orbital pictures shown in Figure 3, one can see that the MOs of Al_7^+ are very similar to those of the reported Al_6^{2-} by Kuznetsov et al.,[20] except that the ordering is slightly different. In addition, the NICS(0) value is as large as -74.17 ppm at the caged center of Al_7^+ (Table 3) and is comparable to the -80.06 ppm of Al_6^{2-}. The HOMO is a multicentered σ-type orbital consisting of the 3p orbitals of all atoms (i.e., head-to-head overlap), which renders Al_7^+ a three-dimensional σ aromatic structure with a large NICS value of -8.46 ppm (Figure 3). The HOMO $-$ 2 is a π-bonding MO and provides π aromaticity. The electron delocalization in Al_7^+ results in bond length equalization and a larger binding energy than in Al_7.

TABLE 3: Nucleus-Independent Chemical Shift (NICS) Values[a](ppm) of Clusters

	Al_3^-	Al_7^+	Al_8O
NICS(0)	-34.67	-74.17	-73.28
NICS(1)	-26.85		

[a] Calculated at the GIAO/6-311G(2d) level.

As for Al_3^-, $RE(Al_7^+)$ can be obtained as

$$RE(Al_7^+) = \Delta E(Al_7^+ \rightarrow 7Al - e^-) - 3\Delta E[Al_2(^1\Sigma_g) \rightarrow 2Al] \quad (3)$$

The value of $RE(Al_7^+)$ calculated by eq 3 is 129.6 kcal/mol, which is about 1.6 times the value of $RE(Al_3^-)$ according to the same definition. In terms of $\Delta E(Al_7^+ \rightarrow 6Al + Al^+)$ and $\Delta E[Al_2(^3\Pi_u) \rightarrow 2Al]$, we obtained the $RE(Al_7^+)$ value as 246.3 kcal/mol. The two $RE(Al_7^+)$ values as the lower and upper limits correspond to a large energy difference between Al^+ and Al.

Among small aluminum clusters, it is known that Al_3^-, Al_4^{2-}, and Al_6^{2-} have multiple aromacities.[17−20] In this work, we found that Al_7^+ has a large NICS value, a large resonance energy, and a high hardness. In addition, Al_7^+ has valence orbitals similar to those of Al_6^{2-}. On the other hand, we note from the geometrical viewpoint that the bond lengths of Al_7^+ are not completely equal, as compared to those of Al_3^-, Al_4^{2-}, and Al_6^{2-}. Al_7^+ has three different bond lengths of 2.605, 2.61, and 2.755 Å (Figure 1), among which the largest deviation is 0.15 Å. In view of the calculated results and the above discussion,

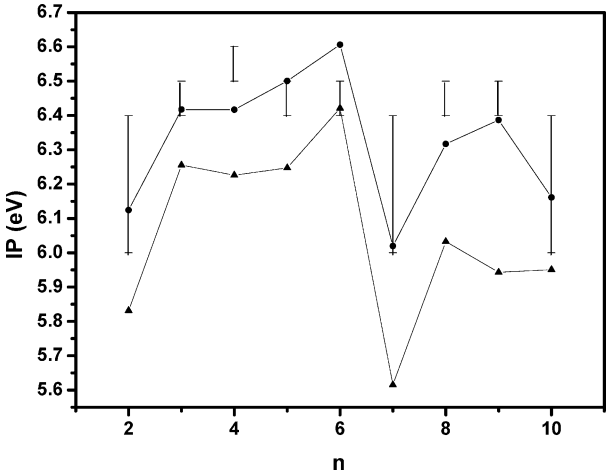

Figure 4. Comparison of experimental (ref 24) (bars) and theoretical ionization potentials for both vertical (circles joined by solid line) and adiabatic (triangles joined by solid line) ionization calculations.

Al_7^+ could be expected to be an aromatic cluster, although it might not be considered as a perfect aromatic system because its bond lengths are not completely equal with each other.

For Al_5^+, a stable planar structure for the triplet state has been reported.[6] In our work, two different spin states are considered for planar Al_5^+, in which the triplet stable structure was obtained, and singlet Al_5^+ is shown to have imaginary frequencies. Our calculated structure of Al_5^+ in the singlet state is a three-dimensional (3D) structure, as shown in Figure 1, that is 0.097 and 0.154 eV lower in energy than the triplet states of the 3D and planar[6] structures, respectively.

As shown in Table 2, the binding energies of Al_2^+, Al_7^+, Al_9^+, and Al_{10}^+ are larger than those of their neutral clusters. This result can be analyzed from two aspects. First, these four clusters are relatively more stable among the studied cationic clusters (Figure 2b), corresponding to the fact that the adiabatic ionization potentials for the neutral Al_n ($n = 2$, 7, 9, and 10) clusters are comparatively small, and thus, they can easily lose one electron to form stable cationic clusters. We can see that, in Al_7^+ and Al_9^+, one bridging bond in the neutral clusters is broken, leading to a more relaxed structure for the cationic clusters. According to steric effects, such structural relaxation might possibly result in a better stability. Second, Al^+ is 6.022 eV higher in energy than Al, and such a large energy difference between Al^+ and Al might also contribute to the large binding energies of Al_2^+, Al_7^+, Al_9^+, and Al_{10}^+.

(iii) Ionization Potential. The vertical ionization potential (vIP) is the difference in energy between the ground state of the neutral cluster and the ionized cluster that has the same geometry as the neutral cluster. Our calculated vIPs are in very good agreement with experimental results,[24] as plotted in Figure 4 and listed in Table 4. The trend of the vIP results are also consistent with the corresponding values reported by Rao et al.[6] There is a maximum at Al_6 and a sharp minimum at Al_7. The vIP of Al_7 is 6.02 eV, which is the lowest among our investigated clusters, and this result can be illustrated by its shell structure of valence electrons. Because Al_7 has one electron beyond the shell-closing requirement, it is easy to lose one electron to form Al_7^+. The adiabatic ionization potentials are also computed from neutral and cationic total energies and are listed in Table 4. Compared with the corresponding vIP, the aIP is always smaller, and the energy difference between them is an indication of the structural relaxation of cationic clusters.

(iv) Electron Detachment Energies. To study the vertical electron detachment energies (VDEs), we have calculated the

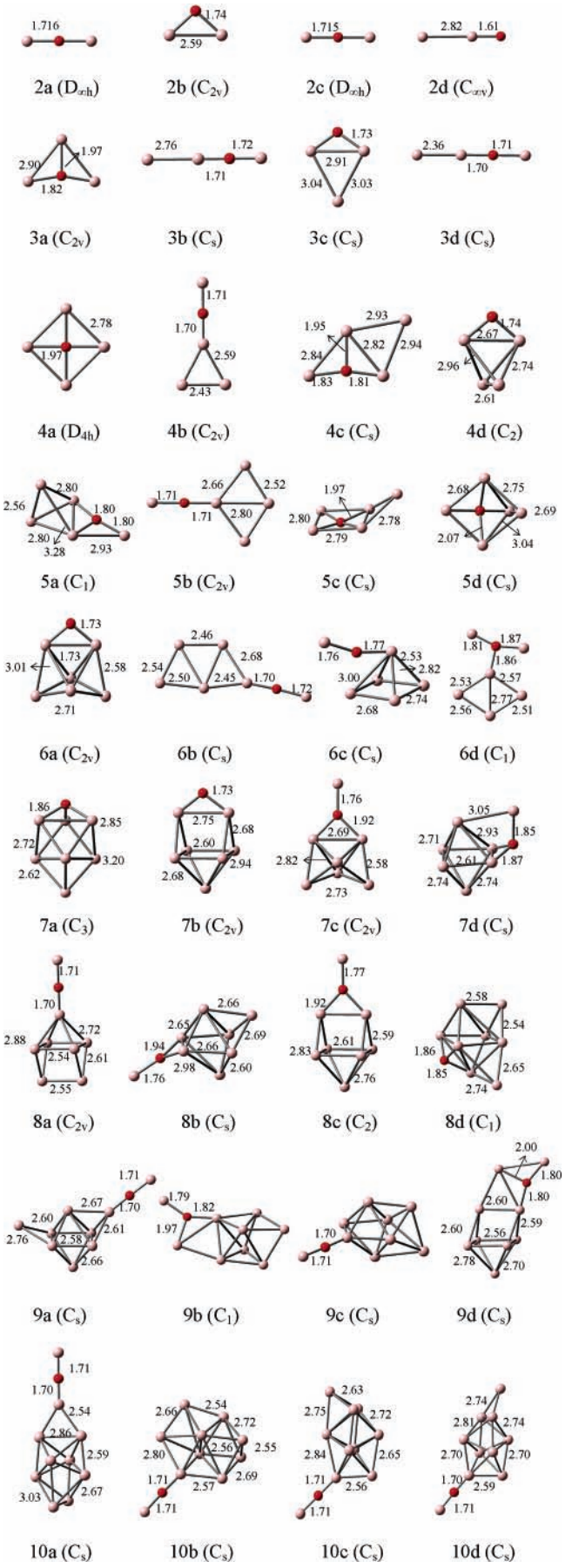

Figure 5. Stable geometries and symmetric point groups of $Al_{2-10}O$ clusters (bond lengths in Å).

TABLE 4: Ionization Potentials of Al_n Clusters and Electron Detachment Energies of Al_n^- Clusters ($n = 2-10$)

	ionization potential (eV)			electron detachment energy (eV)				
n	adiabatic[a]	vertical[a]	expt[b]	adiabatic[a]	expt[c]	vertical[a]	expt[d]	expt[e]
2	5.83	6.12	6.0−6.42	1.27		1.39	1.60	1.46 ± 0.01
3	6.26	6.42	6.42−6.5	1.59	1.53	1.59	1.90	1.89 ± 0.04
4	6.23	6.42	≳6.5	2.03	1.74	2.03	2.20	2.20 ± 0.05
5	6.25	6.50	6.42−6.5	2.02	1.82	2.08	2.30	2.25 ± 0.05
6	6.42	6.61	6.0−6.42	2.26	2.09	2.54	2.65	2.63 ± 0.06
7	5.62	6.02	6.0−6.42	2.01	1.96	2.32	2.50	2.43 ± 0.06
8	6.03	6.32	∼6.42	2.12	2.22	2.38	2.40	2.35 ± 0.08
9	5.94	6.39	≲6.42	2.53	2.47	2.71	2.90	2.85 ± 0.08
10	5.95	6.16	5.9−6.42	2.41	2.47	2.64	2.80	2.70 ± 0.07

[a] Calculated at the B3LYP/6-311G(2d) level. [b] Reference 24. [c] Reference 15. [d] Reference 11. [e] Reference 16.

total energies of Al_n neutral clusters with the geometry of Al_n^-. The calculated VDE results for Al_n^- as well as the corresponding experimental values are listed in Table 4. From Table 4, we can see that our VDE results are all appreciably underestimated, but the trend is in good agreement with the experimental results.[11,16] The adiabatic electron detachment energies (ADEs) are the differences in total energy between the ground states of the anion and the neutral clusters. The results are in good agreement with experiments[15] and theory.[6] At the very high level of CCSD(T)/aug-cc-PV*x*Z (x = D, T, and Q), Zhan et al.[18] calculated the ADEs using complete basis set energies (E_{CBS}) of extrapolations for Al_2^- (1.51 eV), Al_3^- (1.89 eV), and Al_4^- (2.18 eV), obtaining values that are in good agreement with the experimental data from Cha et al.[11] for Al_2^- (1.60 eV), Al_3^- (1.90 eV), and Al_4^- (2.20 eV), as well as those from Li et al.[16] for Al_2^- (1.46 ± 0.01 eV), Al_3^- (1.89 ± 0.04 eV), and Al_4^- (2.20 ± 0.05 eV). For Al_{2-4}^-, our calculated ADEs at the B3LYP/6-311G(2d) level are 1.27, 1.59, and 2.03 eV, respectively, which are lower than the calculated values at the high levels of Zhan et al. Compared to the experimental data,[11,15,16] the ADEs at the B3LYP/6-311G(2d) level are also lower; however, they seem to be relatively close to the experimental data for Al_3^- (1.53 eV) and Al_4^- (1.74 eV) from ref 15. For Al_n^- ($n = 5-10$), the calculated ADEs at the B3LYP/6-311G-(2d) level are 2.02, 2.26, 2.01, 2.12, 2.53, and 2.41 eV, respectively, consistent with the experiment data[15] for Al_5^- (1.82 eV), Al_6^- (2.09 eV), Al_7^- (1.96 eV), Al_8^- (2.22 eV), Al_9^- (2.47 eV), and Al_{10}^- (2.47 eV). Note that ADEs are smaller than VDEs, and the calculated values of the ADEs and VDEs for anionic Al_{2-4} clusters are very close because of their very similar structures.

(v) Hardness. We can also discuss the stability of these clusters on the basis of their hardness. In a finite-difference approximation, DFT has provided a rational for the definition of hardness

$$\eta = \mathrm{IP} - \mathrm{EA} \qquad (2)$$

where IP is the vertical first ionization potential and EA is the vertical electron affinity.[53] Harbola et al. concluded that magic numbers appear at those points where the cluster hardness has a local maximum.[54] From the values listed in Table 2, one can see that magic Al_7^+ has a very large hardness. For the studied neutral and ionic clusters, hardness decreases with cluster size. Martínez et al. [9] calculated the hardness values for Al_n^+ ($n = 1-6$), and our corresponding results are in agreement with theirs.

(B) Al_nO Clusters. *(i) Geometry Optimization.* In Figure 5, we present the stable structures and symmetrical point groups of $Al_{2-10}O$ clusters. The oxygen atom is adsorbed in three ways, i.e., bonding to a single Al atom, bonding to two Al atoms, and bonding to three Al atoms. To locate the lowest-energy structures, several spin multiplicities and initial structures are considered. The optimized structures show that oxygen tends to either be adsorbed at the surface of the aluminum clusters or be inserted between Al atoms to form an $Al_{n-1}OAl$ motif, in which the "Al_{n-1}" part retains the stable structure of pure aluminum clusters. The O coordination numbers are 2, 3, and 4, and the Al−O bond lengths increase correspondingly in the range 1.7−2.0 Å. The Al−Al bond lengths are in the range of 2.56−3.28 Å and show equalization with larger cluster sizes. In structures of amorphous aluminum oxides, according to experimental[55] and theoretical[56,57] studies, most Al atoms have a coordination number of 4, and most O atoms have a coordination number of 3. For the Al_nO ($n = 2-10$) clusters, the coordination numbers are 4 and 5 for most Al atoms and 2 and 3 for most O atoms, consistent with previous studies.

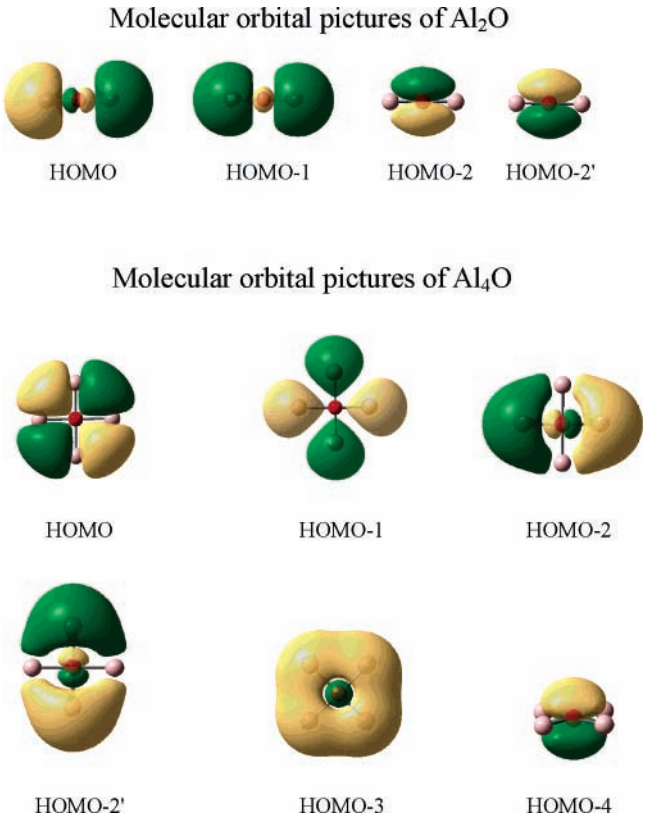

Figure 6. Molecular orbitals of Al_2O and Al_4O (isodensity value is 0.02).

(ii) Energies and Stability. The stability of Al_nO ($n = 2-10$) clusters is discussed in terms of the binding energy (E_b), the binding energy of oxygen [E_b(O)], and the second difference

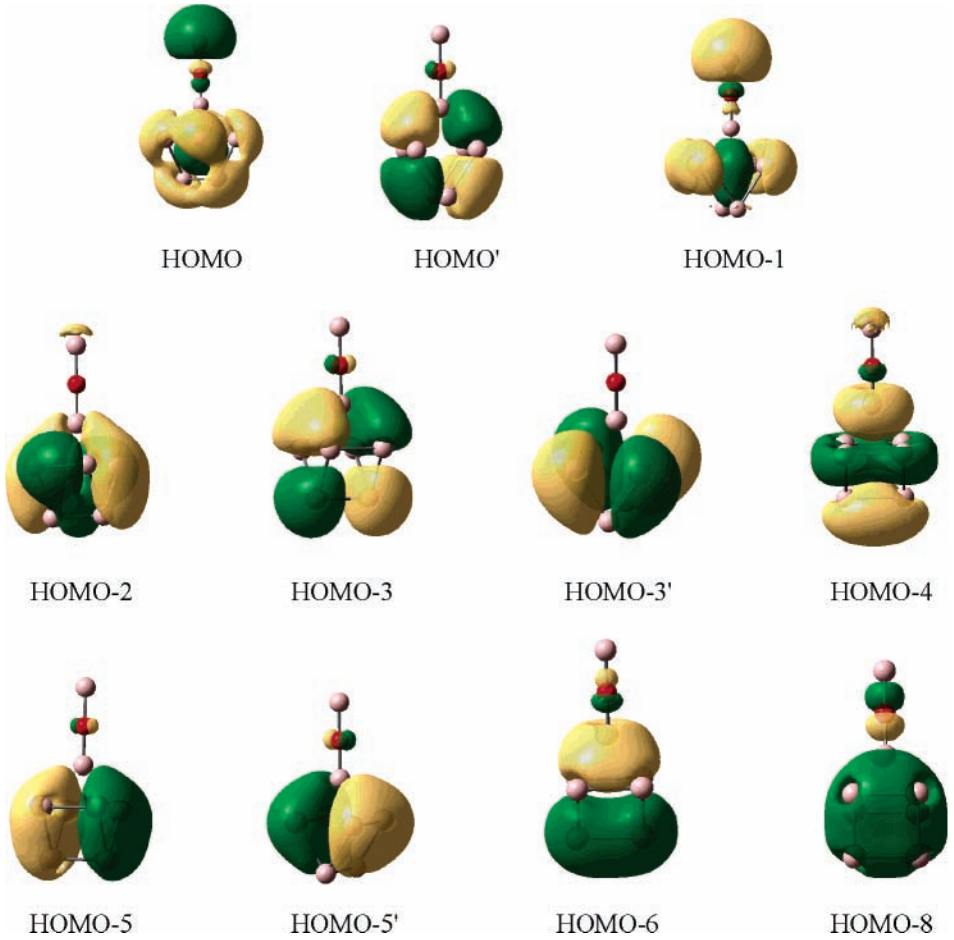

Figure 7. Molecular orbitals of Al_8O (isodensity value is 0.02).

in the total energies (Δ^2E), which are defined as follows

$$E_b = [nE(Al) + {}^1/_2E(O_2) - E(Al_nO)]/(n+1) \quad (3)$$

$$E_b(O) = E(Al_n) + {}^1/_2E(O_2) - E(Al_nO) \quad (4)$$

$$\Delta^2E(Al_nO) = E(Al_{n-1}O) + E(Al_{n+1}O) - 2E(Al_nO) \quad (5)$$

The E_b, $E_b(O)$, and Δ^2E values of $Al_{2-10}O$ clusters are plotted in Figures 8 and 9, and the corresponding data are reported in Table 5. The curve of results shows that Al_2O is very stable and the cluster stability has an odd/even alternation phenomenon along with cluster size.

Al_2O. Al_2O was carefully investigated in early experimental[30,31,58] and theoretical[33] studies. Our calculated **2a** isomer is identified as a linear geometry in the singlet state and is in good agreement with Boldyrev et al.'s structure.[21] It exhibits a prominent peak in Figure 8 and has a large difference (2.865 eV) in total energy relative to **2b**. **2c**, in the triplet state and with a shorter Al−O bond than **2a**, is about 3.284 eV higher in total energy than **2a**.

Al_3O. The lowest-energy isomer, **3a**, is a planar structure with C_{2v} symmetry. The structure was reported by Martínez et al.,[35] whose optimized Al_3O structure at the B3LYP/6-311+G(2d,p) level is quite similar to that of **3a**. At the HF/6-31G* level, the form is a saddle point on the intramolecular rearrangement of Al_3O.[21] The artificially built **3b** can be viewed as an Al atom attached to Al_2O or as an AlO unit attached to Al_2. For $Al_3O \rightarrow Al + Al_2O$ and $Al_3O \rightarrow AlO + Al_2$, the calculated fragmentation energies are 0.632 and 1.484 eV, respectively, showing that Al_3O is easier to dissociate into $Al + Al_2O$ than into $AlO + Al_2$.

Al_4O. The lowest-energy isomer is planar and has D_{4h} symmetry, which is from an O adsorption at the Al_4 center. This structure is in full agreement with Boldyrev and Schleyer's result at the MP2(full)/6-31G* level.[21] Their search strategy employed a fragment approach. The stable structure was obtained with O^{2-} lying in the center of the Al_4^{2+} cluster with D_{4h} symmetry. This contrasts with the usual situation in which the only bonding interactions are between the center atom and its attached atoms or ligands, where the ligand−ligand interactions are repulsive. Hence, usual valence theory does not give a complete explanation.

Al_5O. We find the **5a** structure to be best of all. Although the **5b** with C_s symmetry is a local minimum, it is 0.252 eV higher in total energy than **5a**. **5a** is likely to be most stable, because its "Al_4" part is a stable structure that is beneficial to electronic motion.[4]

Al_6O. The **6a** and **6b** forms have nearly the same energy, but the HOMO−LUMO gap of **6a** is 0.49 eV larger than that of **6b**. From the structures, we can see that the C_{2v} Al_6O is more compact. To confirm stability, we calculated single-point energies at the CCSD(T)/6-311+G(2df) level for both **6a** and **6b**. Indeed, at a high level, **6a** is still 0.275 eV lower in energy than **6b**.

Al_7O. Al_7 has the lowest reactivity that has been observed in experiment.[17,18] We note that the binding energy of O to Al_7 is lowest and the binding energies of isomers **7a**−**7d** are smallest, falling in the range between 4.081 and 3.789 eV (Table 5). Interestingly, after an O atom has been attached to Al_7, the **7a**,

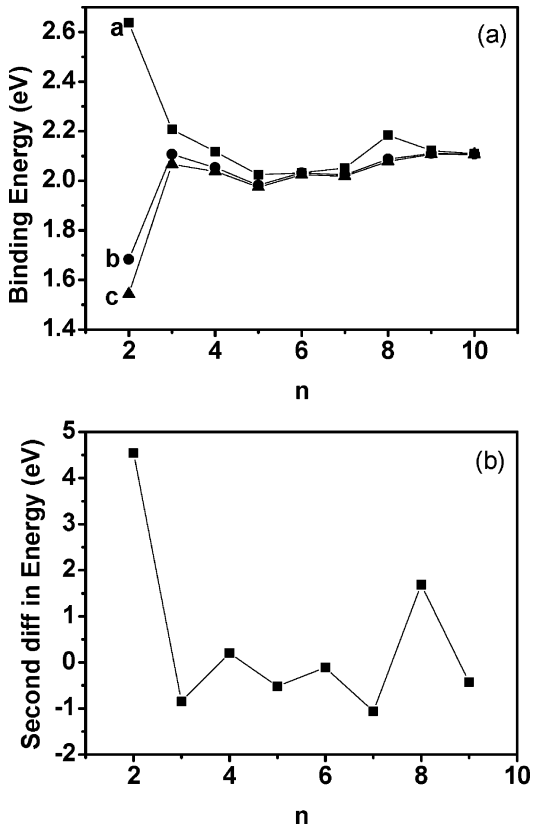

Figure 8. (a) Binding energies of a−c Al_nO isomers and (b) second difference in energies of the lowest-energy Al_nO clusters.

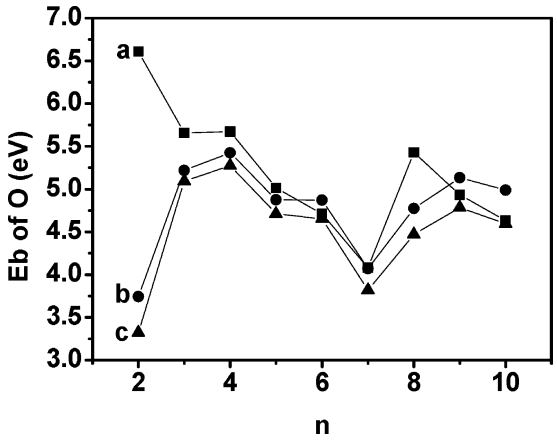

Figure 9. Oxygen binding energies of a−c Al_nO ($n = 2-10$) isomers.

7b, and **7d** structures are compact, and none of the Al atoms moves outward, as compared to the Al_7 structure.

Al_8O. Al_8 would be favored to react with oxygen. Isomers **a**−**c** of Al_8O (Figure 5) can be viewed as an AlO^- unit attached to different sites of Al_7^+. The total energy is obviously lower for **8a** than for the three other isomers, and the HOMO−LUMO gap (Figure 10) is conspicuously large. This structure might be most stable among the isomers of Al_8O, because of the bonding mode that is beneficial to electronic delocalization.

Al_9O. As shown in Figure 5, the lowest-energy structure for oxygen adsorption on Al_9 has a motif similar to Al_8−OAl, as expected. In structure **9a**, the "Al_8" part is distorted: when we tried to draw the tilted atom down and make it similar to Al_8, the atom went back after optimization. We note that the binding energies of **9a** are large in odd-numbered clusters. Thus, Al_9 would be favored to react with oxygen. This is consistent with the experimental results of Cox et al.[24]

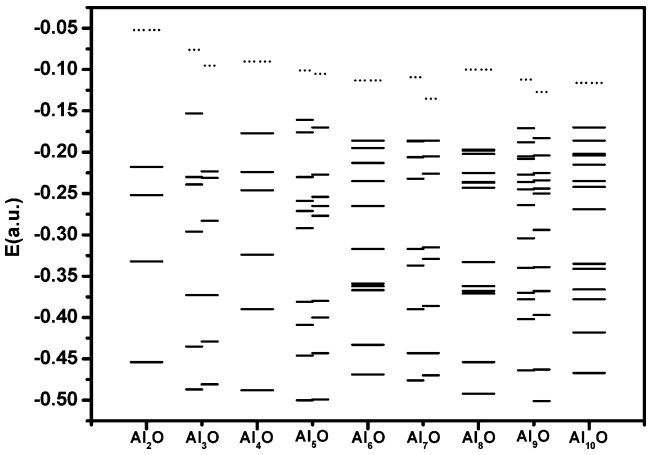

Figure 10. Energy diagram of lowest-energy Al_nO clusters. The dashed lines show the unoccupied states.

$Al_{10}O$. Al_{10} has a chemical stability that makes it less reactive with oxygen, consistent with the experimental results.[24] For the present $Al_{10}O$ isomers, the energies and the HOMO−LUMO gaps are close, and the calculated binding energies of O to Al_{10} are smaller than 4.632 eV, which is only larger than that of Al_7O.

In summary, the binding energies of an O atom adsorbed on Al clusters have a maximum at Al_2O, followed by a decrease with increasing cluster size, minima appearing at Al_7O and $Al_{10}O$, and a prominent increase at Al_8O (Figure 9). The trend is almost consistent with the plot of the rate constant of oxygen adsorbing on Al_n reported by Cox et al.[24]

From the thermodynamic viewpoint, the stability of the lowest-energy clusters can be studied further in terms of the fragmentation energies (Table 6). We have studied all fragmentation channels. The channels leading to Al_2O, Al, or O require the lowest, second lowest, and highest fragmentation energies, respectively. The ground-state energy of AlO is −317.661 au, and the binding energy is 1.228 eV, which is smaller than those of the other clusters. Infrared spectroscopy studies have shown that AlO has a weak bond,[30] so the channel from Al_nO to AlO is not favorable. Instead, Al_nO ($n = 2-10$) clusters are found to preferentially fragment to $Al_2O + Al_{n-2}$.

According to Al_nO ($n = 2-10$) fragmentation energies, Al_2O and Al_8O show the largest stabilities. Al_2O has two fragmentation channels, leading to $Al_2 + O$ and $AlO + Al$, with fragmentation energies of 9.251 eV (213.3 kcal/mol) and 5.459 eV (125.9 kcal/mol), respectively. Our calculated fragmentation energies of 213.3 and 125.9 kcal/mol are in good agreement with the corresponding experimental values, 210.3 ± 4.0 and 127.6 ± 2.0.[59] The fragmentation energies of Al_8O to $Al_2O + Al_6$ and $Al_7O + Al$ are 2.229 and 3.246 eV, respectively, which are the largest in the corresponding channels for Al_nO ($n = 2-10$) clusters except for Al_2O. For the channel $Al_8O \rightarrow Al_8 + O$, the fragmentation energy corresponds to a local maximum. On the other hand, fragmentation of Al_3O into $Al + Al_2O$ has the lowest fragmentation energy among the Al_nO ($n = 2-10$) clusters.

(iii) Electronic Properties. For the lowest-energy isomers of $Al_{2-10}O$, the HOMO−LUMO gaps decrease with increasing cluster size, except for Al_8O (Figure 10). Al_2O has the largest HOMO−LUMO gap of 9.388 eV, and its vIP value is as large as 7.96 eV. In Figure 6, the MOs of Al_2O contain two three-center π bonds that make the AlOAl structure tighter and more stable. In addition, the stability of AlOAl can also be attributed to the fact that the oxygen atom can get two electrons from

TABLE 5: Total Energies E_n (a.u.), Binding Energies E_b (eV), and Binding Energies of Oxygen E_b(O) (eV) of Neutral, Cationic, and Anionic $Al_{2-10}O$ Clusters[a]

structure	E_n	E_b	E_b(O)	structure	E_n	E_b	E_b(O)
2a	**−560.2462587**	2.638	6.609	**6c**	**−1530.0215136**	4.652	6.014
2b	**−560.1409797**	1.683	3.744	**6d**	**−1530.0184532**	4.569	5.388
2c	**−560.125566**	1.543	3.324	**7a**	**−1772.4903972**	4.081	5.415
2d	**−560.1184274**	1.479	3.130	**7b**	**−1772.4824130**	3.864	5.714
3a	**−802.6662791**	2.208	5.657	**7c**	**−1772.4807616**	3.819	5.796
3b	**−802.6515147**	2.107	5.218	**7d**	**−1772.4796499**	3.789	5.878
3c	**−802.6455776**	2.067	5.094	**8a**	**−2014.9960614**	5.429	6.395
3d	**−802.6060097**	1.798	4.017	**8b**	**−2014.9640536**	4.558	5.823
4a	**−1045.1173223**	2.118	5.673	**8c**	**−2014.9608465**	4.471	5.986
4b	**−1045.1054809**	2.054	5.425	**8d**	**−2014.9593849**	4.431	5.388
4c	**−1045.1027212**	2.039	5.276	**9a**	**−2257.4397786**	4.934	5.714
4d	**−1045.0902345**	1.971	4.936	**9b**	**−2257.4354053**	4.815	6.068
5a	**−1287.5609537**	2.025	5.014	**9c**	**−2257.4343147**	4.785	5.850
5b	**−1287.5517065**	1.983	4.876	**9d**	**−2257.4341673**	4.781	5.959
5c	**−1287.5497965**	1.974	4.710	**10a**	**−2499.8992328**	4.632	5.225
5d	**−1287.5469728**	1.961	4.634	**10b**	**−2499.8984688**	4.611	5.197
6a	**−1530.0236771**	2.032	4.711	**10c**	**−2499.8978375**	4.594	5.197
6b	**−1530.0236494**	2.032	4.710	**10d**	**−2499.8968669**	4.567	5.197

[a] Calcluated at the B3LYP/6-311G(2d) level, including zero-point corrections.

TABLE 6: Fragmentation Energies[a] of the Lowest-Energy $Al_{2-10}O$ Clusters

n	$Al_2O + Al_{n-2}$	$Al_{n-1}O + Al$	$AlO + Al_{n-1}$	$O + Al_n$
2		5.459	5.459	9.251
3	0.916	0.916	5.069	8.300
4	1.370	1.760	4.962	8.316
5	1.061	1.558	4.776	7.656
6	1.395	2.078	4.636	7.353
7	1.364	2.186	4.442	6.724
8	2.229	3.246	4.872	8.071
9	0.974	1.561	4.534	7.576
10	1.064	1.989	4.467	7.274

[a] Fragmentation energy is defined by $E(Al_{n-m}O_{1-k}) + E(Al_mO_k) - E(Al_nO)$, and calculated at the B3LYP/6-311G(2d) level.

two Al atoms, i.e., $Al^+O^{2-}Al^+$, and each Al atom can lose an electron to form a closed shell.[21] Thus, the Al atoms can also be considered as monovalent.[6]

For Al_nO ($n \geq 3$), the bonding situation for an O atom with coordination number 3 or 4 is different from that with coordination number 2. As O has two negative charges, the aluminum valences are smaller than that when the O atom has more than two Al atom neighbors. As shown in Figure 6, the HOMO and HOMO − 3 for Al_4O can be regarded as σ MOs as far as the type of the overlaps between the neighboring Al atoms.[18] Here, the bonding interaction between Al atoms plays an important role in stability. In addition, we can also see that the two σ MOs are delocalized σ bonds, and certainly, delocalization can lead to greater stability for electron-lacking systems.

The HOMO−LUMO gap of Al_8O has a local maximum 5.429 eV. Compared to Al_7^+, the MOs of Al_8O include all MOs of Al_7^+, e.g., HOMO and HOMO − 2 of Al_7^+ correspond to HOMO and HOMO − 4 of Al_8O (Figure 7), respectively. Thus, Al_8O can have σ and π aromaticity. For Al_8O, the NICS value is −72.13 ppm at the center, which is close to the value for Al_7^+. This is likely to result in a special stability for Al_8O.

Our natural population analysis (NPA) results for the lowest-energy aluminum oxide species are summarized in Table 7. NPA clearly shows the ionic character of the Al−O bond in these clusters, in which the O atom attracts 1.42−1.64 e− charges from its neighboring Al atom. The charge distribution is dependent on the symmetry of the cluster. We also checked natural bond orbitals. The calculated nonorthogonal natural atomic overlap populations between Al and Al are larger than those between Al and O. Our results agree with the data reported by Boldyrev et al.[21] It might be expected that Al−Al interactions are largely responsible for the larger stability of aluminum oxides.

Conclusions

Using the density functional method, the stable structures of neutral, cationic, and anionic clusters of Al_n ($n = 2-10$) were studied. The structures of Al_5^+, Al_9^+, Al_9^-, Al_{10}, Al_{10}^+, and Al_{10}^- are the new ones that have not been proposed in previous literature reports. The calculated results indicate that the binding energies of clusters increase with the cluster size. For a correlation of stability, neutral clusters have an odd/even alternation phenomenon, and Al_3 and Al_7 clusters have unusual stability because of their electronic structures, which are similar to those of aromatic Al_3^- and Al_7^+, respectively. Our calculated ionization potentials and electron detachment energies (both vertical and adiabatic) are in good agreement with experimental and previous calculated results.

TABLE 7: Natural Charges Populations of the Lowest-Energy $Al_{2-10}O$ Clusters

n	O	Al-1	Al-2	Al-3	Al-4	Al-5	Al-6	Al-7	Al-8	Al-9	Al-10
2	−1.60	0.80[a]	0.80[a]								
3	−1.64	0.31[a]	0.66[a]	0.66[a]							
4	−1.61	0.40[a]	0.40[a]	0.40[a]	0.40[a]						
5	−1.56	0.57[a]	−0.21	0.28	0.78[a]	0.14					
6	−1.42	0.82[a]	−0.11	0.00	0.83[a]	0.00	−0.10				
7	−1.50	−0.07	−0.07	0.60[a]	0.60[a]	0.60[a]	−0.08	−0.07			
8	−1.49	−0.05	0.76[a]	−0.03	0.04	0.02	−0.05	−0.03	0.83[a]		
9	−1.49	-0.08_5	−0.18	−0.18	0.11	−0.16	-0.08_5	0.88[a]	0.83[a]	0.35	
10	−1.50	−0.20	−0.13	0.27	-0.12_5	0.05	−0.20	-0.12_5	0.07	1.07[a]	0.83[a]

[a] Atoms bonding to O atom.

We have further performed systematic study on the Al_nO ($n = 2-10$) clusters. The stable structures were obtained in our exhausting search. The results can be summarized as follows: (1) After an O atom is attached to an Al_n cluster, the resulting structures show that oxygen tends to be absorbed at the surface of the aluminum clusters or to be inserted between Al atoms. The latter corresponds to the process $Al_n + O \rightarrow Al_{n-1}OAl$, in which the structures of the "Al_{n-1}" part are close to those of the corresponding neutral Al_{n-1} clusters. (2) For the lowest-energy Al_nO isomers, the correlation of stability presents an odd/even alternation opposite to the stability of pure aluminum clusters. (3) We find that the Al_2 and Al_8 clusters would mostly favor reaction with oxygen, whereas Al_7 and Al_{10} are less reactive with oxygen, in good agreement with experiments. (4) NPA clearly shows the ionic character of the Al−O bond in these clusters and indicates that Al−Al interactions are largely responsible for the greater stability of aluminum oxides. We hope that this work might be helpful for further experimental and theoretical studies on the mechanism of formation of aluminum clusters and aluminum oxides.

Acknowledgment. This work was supported by the National Natural Science Foundation of China (Nos. 20473030, 20333050, 20073014), Doctor Foundation of the Ministry of Education, Foundation for University Key Teachers of the Ministry of Education of China, and Foundation of Innovation by Jilin University.

References and Notes

(1) Jia, J. F.; Wang, J. Z.; Liu, X.; Xue, Q. K.; Li, Z. Q.; Kawazoe, Y.; Zhang, S. B. *Appl. Phys. Lett.* **2002**, *80*, 3186.
(2) Trost, J.; Brune, H.; Wintterlin, J.; Behm, R. J.; Ertl, G. *J. Chem. Phys.* **1998**, *108* (4), 1740.
(3) Jones, R. O. *Phys. Rev. Lett.* **1991**, *67*, 224.
(4) Jones, R. O. *J. Chem. Phys.* **1993**, *99*, 1194.
(5) Yang, S. H.; Drabold, D. A.; Adams, J. B.; Sachdev, A. *Phys. Rev. B* **1993**, *47*, 1567.
(6) Rao, B. K.; Jena, P. *J. Chem. Phys.* **1999**, *111*(5), 1890.
(7) Bergeron, D. E.; Castleman, A. W., Jr.; Morisato, T.; Shiv Khanna, N. *Science* **2004**, *304*, 84.
(8) (a) Bauschlicher, C. W., Jr.; Partridge, H.; Langhoff, S. R.; Taylor, P. R.; Walch, S. P. *J. Chem. Phys.* **1987**, *86*, 7007. (b) Bauschlicher, C. W., Jr.; Barnes, L. A.; Taylor, P. R. *J. Phys. Chem.* **1989**, *93*, 2932.
(9) Martínez, A.; Vela, A. *Phys. Lett. B* **1994**, *49*, 17464.
(10) Martínez, A.; Vela, A.; Salahub, D. R. *Int. J. Quantum Chem.* **1997**, *63*, 301.
(11) Cha, C.-Y.; Gantefr, G.; Eberhardt, W. *J. Chem. Phys.* **1994**, *100*, 995.
(12) Hettich, R. L. *J. Am. Chem. Soc.* **1989**, *111*, 8582.
(13) Hanley, L.; Ruatta, S.; Anderson, S. *J. Chem. Phys.* **1987**, *87*, 260.
(14) Jarrold, M. F.; Bower, J. E.; Kraus, J. S. *J. Chem. Phys.* **1987**, *86*, 3876.
(15) Taylor, K. J.; Pettiette, C. L.; Graycraft, M. J.; Chesnovsky, O.; Smalley, R. E. *Chem. Phys. Lett.* **1988**, *152*, 347.
(16) Li, X.; Wu, H.; Wang, X. B.; Wang, L. S. *Phys. Rev. Lett.* **1998**, *81*, 1909.
(17) Li, X.; Kuznetsov, A. E.; Zhang, H.-F.; Boldyrev, A. I.; Wang, L.-S. *Science* **2001**, *291*, 859.
(18) Zhan, C.-G.; Zheng, F.; Dixon, D. A. *J. Am. Chem. Soc.* **2002**, *124*, 14795.
(19) Kuznetsov, A. E.; Boldyrev, A. I. *Struct. Chem.* **2002**, *13*, 141.
(20) Kuznetsov, A. E.; Boldyrev, A. I.; Zhai, H.-J.; Li, X.; Wang, L.-S. *J. Am. Chem. Soc.* **2002**, *124*, 11791.
(21) Boldyrev, A. I.; Schleyer, P. v. R. *J. Am. Chem. Soc.* **1991**, *113*, 9045.
(22) Leuchtner, R. E.; Harms, A. C.; Castleman, A. W. *J. Chem. Phys.* **1990**, *94* (2), 1093.
(23) Cooper, B. T.; Parent, D.; Buckner, S. W. *Chem. Phys. Lett.* **1998**, *284*, 401.
(24) Cox, D. M.; Trevor, D. J.; Whetten, R. L.; Kaldor, A. *J. Phys. Chem.* **1988**, *92*, 421.
(25) Fuke, K.; Nonose, S.; Kikuchi, N.; Kaya, K. *Chem. Phys. Lett.* **1988**, *147*, 479.
(26) Leuchtner, R. E.; Harms, A. C.; Castleman, A. W. *J. Chem. Phys.* **1989**, *91* (4), 2753.
(27) Jarrold, M. F.; Bower, J. E. *J. Chem. Phys.* **1986**, *85*, 5373.
(28) Jarrold, M. F.; Bower, J. E. *J. Chem. Phys.* **1987**, *87*, 1610.
(29) Jarrold, M. F.; Bower, J. E. *J. Chem. Phys.* **1987**, *87*, 5728.
(30) Bamca, S. J.; Haak, M.; Niblcr, J. W. *J. Chem. Phys.* **1985**, *82*, 670.
(31) Andrews, L.; Burkbolder, T. R.; Yustein, J. T. *J. Phys. Chem.* **1992**, *96*, 10182.
(32) Lengsfield, B. H.; Liu, B. *J. Chem. Phys.* **1982**, *77*, 6083.
(33) Masip, J.; Clotet, A.; Ricart, J. M.; Illas, F.; Rubio, J. *Chem. Phys. Lett.* **1988**, *144*, 373.
(34) Martínez, A.; Tenorio, F. J.; Ortiz, J. V. *J. Phys. Chem. A* **2001**, *105*, 8787.
(35) Martínez, A.; Sansores, L. E.; Salcedo, R.; Tenorio, F. J.; Ortiz, J. V. *J. Phys. Chem. A* **2002**, *106*, 10630.
(36) Martínez, A.; Tenorio, F. J.; Ortiz, J. V. *J. Phys. Chem. A* **2001**, *105*, 11291.
(37) Martínez, A.; Tenorio, F. J.; Ortiz, J. V. *J. Phys. Chem. A* **2003**, *107*, 2589.
(38) Gowtham, S.; Lau, K. C.; Deshpande, M.; Pandey, R.; Gianotto, A. K.; Groenewold, G. S. *J. Phys. Chem. A* **2004**, *108*, 5081.
(39) Wu, H.; Li, X.; Wang, X.-B.; Ding, C.-F.; Wang, L.-S. *J. Chem. Phys.* **1998**, *109*, 449.
(40) Desai, S. R.; Wu, H.; Wang, L.-S. *Int. J. Mass Spectrom. Ion Processes* **1996**, *159*, 75.
(41) Campbell, T.; Kalia, R. K.; Nakano, A. *Phys. Rev. Lett.* **1999**, *82*, 4866.
(42) Knight, W. D.; Clemenger, K.; de Heer, W. A.; Saunders, W. A.; Chou, M. Y.; Cohen, M. L. *Phys. Rev. Lett.* **1984**, *52*, 2141.
(43) Frisch, M. J.; Trucks, G. W.; Schlegel, H. B.; Scuseria, G. E.; Robb, M. A.; Cheeseman, J. R.; Zakrzewski, V. G.; Montgomery, J. A., Jr.; Stratmann, R. E.; Burant, J. C.; Dapprich, S.; Millam, J. M.; Daniels, A. D.; Kudin, K. N.; Strain, M. C.; Farkas, O.; Tomasi, J.; Barone, V.; Cossi, M.; Cammi, R.; Mennucci, B.; Pomelli, C.; Adamo, C.; Clifford, S.; Ochterski, J.; Petersson, G. A.; Ayala, P. Y.; Cui, Q.; Morokuma, K.; Malick, D. K.; Rabuck, A. D.; Raghavachari, K.; Foresman, J. B.; Cioslowski, J.; Ortiz, J. V.; Stefanov, B. B.; Liu, G.; Liashenko, A.; Piskorz, P.; Komaromi, I.; Gomperts, R.; Martin, R. L.; Fox, D. J.; Keith, T.; Al-Laham, M. A.; Peng, C. Y.; Nanayakkara, A.; Gonzalez, C.; Challacombe, M.; Gill, P. M. W.; Johnson, B. G.; Chen, W.; Wong, M. W.; Andres, J. L.; Head-Gordon, M.; Replogle, E. S.; Pople, J. A. *Gaussian 03*, revision B.03; Gaussian, Inc.: Pittsburgh, PA, 2003.
(44) (a) Becke, A. D. *J. Chem. Phys.* **1993**, *98*, 5648. (b) Lee, C.; Yang, W.; Parr, R. G. *Phys. Rev. B* **1988**, *37*, 785. (c) Mielich, B.; Savin, A.; Stoll, H.; Preuss, H. *Chem. Phys. Lett.* **1989**, *157*, 200.
(45) Schleyer, P. v. R.; Maerker, C.; Dransfeld, A.; Jiao, H.; Hommes, N. J. R. v. E. *J. Am. Chem. Soc.* **1996**, *118*, 6317.
(46) Wolinski, K.; Hilton, J. F.; Pulay, P. *J. Am. Chem. Soc.* **1990**, *112*, 8251.
(47) Pople, J. *Adv. Chem. Phys.* **1969**, *14*, 35.
(48) Purvis, G. D., III.; Bartlett, R. J. *J. Chem. Phys.* **1982**, *76*, 1910.
(49) Scuseria, G. E.; Janssen, C. L.; Schaefer, H. F., III. *J. Chem. Phys.* **1988**, *89*, 7282.
(50) (a) Glendening, E. D.; Reed, A. E.; Carpenter, J. E.; Weinhold, F. *NBO*, version 3.1. (b) Glendening, E. D.; Weinhold, F. *J. Comput. Chem.* **1998**, *19*, 628.
(51) Minkin, V. I.; Glukhovtsev, M. N.; Simkin, B. Y. *Aromaticity and Antiaromaticity*; Wiley: New York, 1994.
(52) Dewar, M. J. S.; deLlano, C. *J. Am. Chem. Soc.* **1969**, *91*, 789.
(53) Zhan, C.-G.; Nichols, J. A.; Dixon, D. A. *J. Phys. Chem. A* **2003**, *107*, 4184.
(54) Harbola, M. K. *Proc. Natl. Acad. Sci. U.S.A.* **1992**, *89*, 1036.
(55) Lamparter, P.; Kniep, R. *Physica B* **1997**, *405*, 234.
(56) Keen, D. A.; McGreevy, R. L. *Nature (London)* **1990**, *344*, 423.
(57) Gutiérrez, G.; Johansson, B. *Phys. Rev. B* **2002**, *65*, 104202.
(58) Cai, M.; Carter, C. C.; Miller, T. A.; Bondybey, V. E. *J. Chem. Phys.* **1991**, *95*, 73.
(59) Huber, K. P.; Herzberg, G. *Molecular Spectra and Molecular Structure. Constants of Diatomic Molecules*; Van Nostrand Reinhold: New York, 1979.